frontiers | Frontiers in Earth Science

ORIGINAL RESEARCH
published: 15 June 2022
doi: 10.3389/feart.2022.892179

The Piping Failure Mechanism of a Loess Dam: The 2021 Dam Break of the Yang Village Reservoir in China

Wenguo Ma[1,2], *Gang Zhang*[2]*, *Youzhen Yang*[1,2], *Ping Wang*[3], *Yishen Zhao*[1,2] and *Qingqing Lin*[1,2]

[1]School of Physics and Electronic-Electrical Engineering, Ningxia University, Yinchuan, China, [2]Institute of Solid Mechanics, Ningxia University, Yinchuan, China, [3]Key Laboratory of Loess Earthquake Engineering, China Earthquake Administration and Gansu Province, Lanzhou, China

The construction of a reservoir on a large-thickness collapsible loess cover will significantly increase the occurrence of dam break disasters. The main reason may be that although the gradation of loess particle is not uniform. The clay content is less than 10%. Piping channels easily form under the action of force and collapsibility. Near-static liquefaction of the loess in the dam body under the saturated condition will lead to piping or loss of soil strength. Therefore, it is of great significance to study the mechanical characteristics of loess in the saturated state for preventing dam break. The study investigated the 2021 dam failure of the Yang village reservoir in Ningxia, China, which resulted in millions of dollars of property damage but no casualties. The dam break is a gradual development from piping to complete dam break. This study tries to find out the real reason for dam break from the physical and mechanical properties of the foundation and the dam. We mainly carried out the research through the following three aspects: First, the dam structure was identified by using the seismograph, the compactness of the dam foundation and the dam body was determined according to the wave velocity of the soil layer, and the construction quality of the dam foundation and the dam body was comprehensively evaluated. Second, the particle size distribution confirmed the mechanism of uneven particle size distribution and clay loss. Finally, the undrained characteristics of saturated loess are tested, and the dam failure is essentially explained. The research results show that using this loess to fill the dam foundation directly and the dam body has a very high probability of piping-type dam failure. This study gives some design suggestions for using this loess for dam building, for example, through the design of the filter layer to increase the difficulty of piping occurrence.

Keywords: loess, Yang village reservoir, piping failure, dam break, near-static liquefaction

OPEN ACCESS

Edited by:
Candan Gokceoglu, Hacettepe University, Turkey

Reviewed by:
Mustafa Kanık, Firat University, Turkey
Anand Shivapur, Visvesvaraya Technological University, India

***Correspondence:**
Gang Zhang
zhanggang@nxu.edu.cn

Specialty section:
This article was submitted to Geohazards and Georisks, a section of the journal Frontiers in Earth Science

Received: *08 March 2022*
Accepted: *19 April 2022*
Published: *15 June 2022*

Citation:
Ma W, Zhang G, Yang Y, Wang P, Zhao Y and Lin Q (2022) The Piping Failure Mechanism of a Loess Dam: The 2021 Dam Break of the Yang Village Reservoir in China. Front. Earth Sci. 10:892179. doi: 10.3389/feart.2022.892179

INTRODUCTION

By the end of 2021, China has built about 100,000 reservoirs of all types, with a total storage capacity of about 9.0×10^{11} m^3 (Ministry of Water Resources of the PRC, 2021). About 280 reservoirs with a total storage capacity of 1.736×10^8 m^3 have been built in the Loess region of Ningxia. The main functions of reservoirs in Ningxia are irrigation, water supply, and aquaculture. Because of the depth and breadth of loess distribution, local materials are usually needed in the design and construction process of the dam foundation and dam body. Due to the compatibility of loess, the mechanical properties in a saturated state, and the relatively uniform gradation, there are various unpredictable

dam break factors in the design, and construction of reservoir dam failure risk is still an important problem in dam design, construction, and operation.

It is of great significance to learn lessons from the past dam break events and discuss the main rules of dam break for revealing the dam break mechanism of the reservoir and improving the safety management level of the reservoir. International Commission on Large Dams (ICOLD) Bulletin No. 175 extends the traditional method and concept to all stages before the operation stage. Many risks of dam operation come from other steps before the actual operation. This announcement is a first attempt to systematically describing the participants, roles, activities, and complex interactions involved in different stages of the dam life cycle (ICOLD, 2021) and to capture all related dam safety aspects in all preoperation stages. China, the United States, and Australia also conducted statistical analysis of the dam failure data in their own countries and summarized the causes of the dam failure. Since 2016, the average annual dam failure rate of reservoirs in China has been 0.03‰, the lowest in history, which is lower than the world-recognized standard of low dam failure rate of 0.1‰ (Ministry of Water Resources of the PRC, 2021). The United States Society on Dams (USSD) published Dams of the United States- A Pictorial Display of Landmark Dams (USSD, 2013), which introduced the concept and practical experience of dam safety management in the United States, which is worthy of reference and reference for the dam industry. The Australian National Committee on Large Dams Incorporated (ANCOLD) revised the Guidelines on the Consequence Categories for Dams (ANCOLD, 2020). The revised guide classifies potential loss of life (PLL) and the severity of damage and loss. The 6.0 m moraine core rockfill dam and the 4.5 m homogeneous earth dam with a dam height of 4.5 m are the most representative ones carried out by the EU investigation of extreme flood processes and uncertainty (IMPACT) project, the test demonstrates the whole process of dam break caused by piping (Morris et al.,2007). The Gleno dam is located in the Alps in Central Italy. A few days after the first impoundment of the reservoir it suddenly collapsed. The dam released almost 4.5 million cubic meters of water. The floods wreaked havoc in the lower valley, killing 356 people. This is the only event in Italian history when the dam collapsed due to a structural defect. The main information obtained from a large number of historical documents about the dam break of the Gleno Dam produced a dam break model, which is helpful to verify the mountain. (Pilotti et al., 2011). In the United States, the main reason for earth dam failure is flooded overtopping, followed by piping caused by seepage. For example, on 14 May 2014, the Corti-Jensen dam in Virginia had piping due to seepage, causing some dam bodies to burst, but did not cause harm to the downstream (Wu, 2020). Through a series of centrifugal model tests, the barrier lake dams failure process and mechanism due to overtopping are analyzed, and the test process of overtopping failure is simulated (Zhao et al., 2019). The Situ Gintung dam burst on 27 March 2009, according to the evaluation of the Ministry of Public Works, the main reason for the collapse of the dam body is the weakening of the dam body soil, which may be caused by the erosion and cracking of the embankment with the spillway on the left. The water in the reservoir enters the dam body through the cracks and gradually reaches a saturated state, and the shear strength of the soil body decreases (Nabilah et al., 2020). They proposed a dam risk probabilistic model (DRPM) consisting of three factors: hydrology, seepage, and slope instability, and applying this model to the Dongwushi Reservoir in Hebei Province, China, the comprehensive threshold for dam failure of the reservoir are 1.25, which indicates that the dam is in serious danger according to Guidelines On Dam Safety Evaluation of the Ministry of Water Resources of the PRC (2017). By introducing the proposed theory and method into the dam safety evaluation system, dam safety management can be carried out efficiently (Zhonget al., 2011). The BOSS-DAMBRK (this software is developed that is based on hydrodynamic flood routing) software was used to simulate the dam failure, when the entire dam collapsed at once, the extent of the downstream flood, flood propagation time, flood speed, and the impact of flood released by dam structure damage on downstream affected residents, property, and environmentally sensitive areas (Kho et al., 2009; Boss International, 1999). A total of 3,498 dam break cases in China from 1954 to 2006 are collected, and statistics are made from the historical period of a dam break, regional distribution, reservoir scale, dam height, dam type, dam break reason, dam break rate, and other aspects. The causes of the dam break and its main failure modes are preliminarily analyzed (Xie and Sun, 2009). Based on the dam break data of small reservoirs in China from 1980 to 2006, the researchers described the causes and laws of dam break of small reservoirs. They believed that the standardized management of reservoirs and the continuous promotion of reinforcement of dangerous reservoirs had laid a necessary foundation for improving the safety level of small reservoirs (Jiang and Yang, 2008).

Take the Loess dam in the Ansai area, Yan'an City, Shaanxi Province, China, as a monitoring target. The Loess dam is not fully compacted, and there may be a high permeability area in the Loess dam. Seepage channels appear in the dam body, and seepage damage occurs. These events lead to instability and damage to the dam's body. By measuring the crack, liquid level, and pore pressure, the whole life cycle of the dam is monitored. From the beginning of monitoring to the dam failure, the dam experiences three distinct types of failure, which are referred to as "internal erosion damage, slumping damage," and "slippery damage" (Xu et al., 2020a). The research object is a loess accumulation dam in Ansai Area, Yan'an City, Shaanxi Province, China. A triaxial undrained test of saturated remodeled loess was carried out on the dam body. The test shows that the deviatoric stress and pore water pressure of saturated remolded loess increase with the increase of shear strain and gradually approximated the horizontal under different cell pressure. According to on-site monitoring, it can be determined that there is more than three times the apparent damage to the dam. Through the comparison of in-site tests and indoor tests, the concept and calculation method of "inspection threshold" are put forward (Xu, et al., 2020b). Check dam system has been widely used in the Loess Plateau. However, due to the hidden danger of the dam breaking. The development of the

FIGURE 1 | Location of the Yang village reservoir.

check dam system is limited. A hydrodynamic simulation was carried out based on the failure of a typical check dam system on 15 July 2012. The simulation results show that the series fault in the tributary ditch will not lead to the stack of peak discharges. The peak flow at the catchment outlet is 20% higher than that without a dam break and 87% lower than that without a check dam (Zhang et al., 2021c). Check dam system has been widely used in the Loess Plateau. However, due to the hidden danger of the dam breaking. The development of the check dam system is limited. A hydrodynamic simulation was carried out based on the failure of a typical check dam system on 15 July 2012. The simulation results show that the series fault in the tributary ditch will not lead to the stack of peak discharges. The peak flow at the catchment outlet is 20% higher than that without a dam break and 87% lower than that without a check dam (Wang et al., 2021a). The characteristics of earth-rock dam failure research are reviewed, and the results of dam safety management (DSM) are reviewed from three aspects: disaster causes, dam failure process, and flood propagation. To improve the DSM system does not appear to be modifying the subject of the research on the change of the material properties of the dam body and its corresponding effect, the scale effect, the similarity criterion of the dam break process, and the uncertainty analysis of the commonly used models (Luo et al., 2012).

The dam break accident of the reservoir in the loess area has not been fully investigated, but there have been reports. The reasons for the dam break of reservoirs in the loess area are usually only judged based on experience. For example, causes of dam breaks are summarized into natural factors, engineering factors, and human factors, and specific mechanisms and experimental analyses are rarely carried out. This study attempts to analyze the fundamental cause of the dam break of the Yang village reservoir in the Loess Plateau, Ningxia, China, by using mechanical methods: The possibility of piping is judged according to the particle size distribution of the loess. According to the mechanical properties of remodeled saturated loess under undrained conditions, a reasonable explanation for the dam break of the reservoir may be made. The surface wave velocity test is carried out on the top of the dam to judge the compaction inside the dam body. According to the physical and mechanical properties of loess and the undrained triaxial test, the design proposal of anti-seepage and anti-filtration of a dam filled with loess material is put forward.

YANG VILLAGE DAM BREAK

Location and Introduction of Dam Break

This study investigates the failure of a loess-filled reservoir on the Loess Plateau in Ningxia, China, in the spring of 2021. The Yang village reservoir is located in the position shown in **Figure 1**. The reservoir has an area of 40,000 m^2 and a design capacity of 2.0 × 10^5 m^3. When the dam broke, the stored 1.4 × 10^5 m^3 water was washed out. The outline and breach of the reservoir are shown in

FIGURE 2 | Reservoir contour and dam break images in different directions.

FIGURE 3 | Measured length of the south slope of the dam body.

Figure 2, **Figure 2A** shows the outline of the whole reservoir, and **Figures 2B–D** show the front, side, and top views of the dam break, respectively. The breach is on the south side of the dam body, with a width of about 20 m. The sloped body on the south side of the dam body is shown in **Figure 3**, the slope length is 19 m, the inclination angle is 30 degrees, and the filling height of the dam body is 9.5 m. It can be seen from **Figures 2B,C** that the soil moisture content and layer thickness are well controlled during the construction of the dam bodies above the bottom of the breach. The damage of the dam body starts from the seepage at the bottom. It can be seen from **Figure 6** that the wave velocity at the bottom of the dam body is relatively small, corresponding to the same loess filling material, it can be considered that the compaction degree of the dam body bottom is relatively low. Therefore, under the action of the seepage force, the fine particles are gradually brought out of the dam body, and a piping channel is gradually formed at the bottom of the dam, which eventually leads to a complete dam failure. The dam breaks mainly caused nearly 0.67 km^2 of farmland to be flooded, but there were no casualties.

Geological Environment and Dam Compactness

The reservoir is located in the hinterland of the Loess Plateau the west of Hongjian Mountain. The dam foundation is directly built on the thick loess stratum, which is the Q^4 (according to the classification of stratigraphic age, the loess belongs to the sediments of Cenozoic, Quaternary, and Holocene) loess layer with a detectable depth of more than 10 m. The north and west of the reservoir depend on mountains, the south and east dams are filled with loess, and the location of the dam break is just in the dam filled in the south. As can be seen from **Figure 2C** that the

FIGURE 4 | Collection point of the test soil sample.

FIGURE 5 | Geophones arranged along the longitudinal section.

dam break started from the bottom of the dam, and there is no trace of water scouring in the middle and upper part of the dam body. The possible reason is that the compactness of the lower dam body is relatively low. After the geomembrane or geotextile blanket leakage, the water gradually infiltrates into the loess, forming a dominant channel of seepage in the dam body, resulting in the collapse of the whole dam body.

MATERIALS AND METHODS

Physical and Mechanical Properties of Loess

The filling materials in the south of the reservoir are all from the farmland in the dam's south. The farmland in the south is a slope land on the Loess Hill. As shown in **Figure 4**, the soil samples were taken from the western slope, located 3 m above the surface. The loess is massive in the dry state and muddy in the saturated state. The basic physical and mechanical properties of loess were measured in the indoor laboratory. **Table 1** gives the specific gravity, natural density, liquid limit, plastic limit, plasticity index, collapsibility coefficient, and permeability coefficient of soil samples.

Surface Wave Exploration

The Multichannel Analysis of Surface Waves (MASW) is a nondestructive method, which analyzes the dispersion characteristics of Rayleigh waves to determine how the shear wave velocity changes with depth in the layered underground. The surface wave method is widely used in seismic engineering, geotechnical engineering, and geological engineering. (Islam and Chik, 2011; Ismail et al., 2014; Harba et al., 2019). The surface wave method is also widely used in the exploration of the loose soil zone, foundation compactness, underground cavity, and complex shallow geological environment (Karray and Lefebvre, 2009; Khan and Yamin, 2019). To investigate the internal compactness of the Yang village reservoir, we conducted a surface wave test on a section of the dam (the surface wave detectors in **Figure 5** are arranged along the longitudinal section of the fracture. There are 24 detectors in total, and the 17th detector is arranged in the center of the fracture from west to east.) to obtain the details of surface wave velocity at the first 10 m below the surface. During the field investigation, we used the OYO McSEIS-SW high-precision shallow seismic instrument, 24 channels, the frequency of geophones is 4 Hz, the interval between geophones is 2 m, and the wooden hammer is used to excite the surface wave. We ensure that the surface wave excited by each hammer meets the requirements in the test. After the test, we use Seisimager software (McSEIS-SW data post-processing section) to analyze the dam body's wave velocity after filling to judge the dam body's compactness.

Triaxial Test of Loess

The dam body filled with natural loess materials may be partially saturated when the geomembrane or geotextile blanket and other impervious materials are damaged. To determine the mechanical properties of loess in a saturated state, we collected undisturbed and disturbed loess samples from the borrow pit wall on the south

TABLE 1 | Physical and mechanical property parameters of loess samples.

Specific gravity	Natural density	Liquid limit	Plastic limit	Plasticity index	Collapsibility coefficient	Permeability coefficient
G_s	ρ(g/cm^3)	w_L	w_P	I_P	δ_s	k (m/s)
2.7	1.36	27.2	18.2	9	0.056	2.5E-6

side of the reservoir. The remolded soil samples collected on-site are broken with a 2 mm sieve in the laboratory. Because the soil samples on-site are kept wet, the screening and crushing effect is perfect. The screened soil samples are used for particle size analysis and triaxial test. We used Mastersizer 3,000 laser particle sizer to test the particle size of samples by the dry method and the wet method, respectively, and each sample was tested three times. We conducted consolidated undrained (Cu) triaxial compression shear tests on loess samples under two confining pressure (100 and 200 kPa) to study the shear strength, pore water pressure development, and stress path of dam filled loess. The triaxial undrained test in this study is carried out according to ASTM standards (ASTM, 2020) are following:

1) Sample preparation: we prepare a cylindrical soil sample with a 1.5 g per cubic centimeter dry density. The height of the soil sample is 100 mm, and the diameter is 50 mm.
2) Sample installation: we protect the prepared soil sample, install the soil sample on the base of the actuator, lift the base to maintain 5N contact between the soil sample and the upper force sensor, and apply a 30 kPa confining pressure to the soil sample through the pressure–volume controller.
3) Sample saturation: we replace the saturation with carbon dioxide, and use degassed water for head saturation and back pressure saturation. We set the head pressure of 5 kPa for head saturation and keep the back pressure saturation at about 200 kPa, and the b value is more than 0.95.
4) Sample consolidation: the sample is consolidated under the confining pressure of 100 and 200 kPa, respectively. The consolidation standard is that the displacement is 0.1 ml/h, and the consolidation curve hardly changes.
5) Sample shear: we use the strain control method for consolidated undrained shear. The axial strain increases at the rate of 0.01%/min. When the axial strain is close to 20%, terminate the test.

RESULTS

Dam Compactness

Now, as a conventional geophysical exploration method. MASW has been used to determine the dam structure and compactness. MASW is favored because it can distinguish weak layers and better describe the characteristics of shallow soil. The weak penetrating layer may cause the seepage and piping of the dam body. The dam body is a uniform geological body built manually, and the hidden danger is the uneven body (weak interlayer, layered loose zone, and crack) existing in the uniform medium, which is very consistent with the research method of MASW. As we all know, surface waves mainly contain shallow strata information. Hammering waves can detect cracks near the ground, and it is indisputable that surface wave velocity changes are caused by minor faults, subsidence boundaries, cavities, etc., Therefore, in detecting the surface wave velocity changes in a shallow stratum, the surface wave has formed a meaningful primary wave, which should not be simply regarded as noise. The Rayleigh wave velocity of soil is similar to its shear wave velocity, and the shear wave velocity of soil is an important index to evaluate the strength of rock and soil, which is common knowledge. Therefore, if we carry out continuous exploration with the transient Rayleigh wave method along the strike of the earth dam, we can draw the Rayleigh wave velocity profile of the dam body by using the dispersion curve to evaluate the quality of the earth dam. **Figure 6** shows the shear wave velocity distribution on a typical longitudinal profile of the dam body. From **Figure 6**, we can find that the soil density at the dam foundation is still relatively low. In general, there is a good statistical relationship between shear wave velocity and density, for example, the experiments showed that the relationship between shear wave speed and void ratio can be expressed as follows:$V_s = 69\,(2.973 - e)^{5.5}\rho_s^{-0.5}$, where V_s, e, and ρ_s represent shear wave speed, void ratio, and soil particle density, respectively (Wang et al., 2021b).

Particle Size Distribution

The particle size grading curve of dam filling loess is measured by the dry and wet methods, respectively. **Figure 7** shows the particle size grading curve of dam filling of the Yang village reservoir. It can be seen from **Figure 7** that the mass of particles with a particle size of 5~75 um accounts for 88% of the total mass, and the plasticity index is less than 10. Therefore, the loess filling the dam body is typical silt. The non-uniformity coefficient C_u = 5.9 and curvature coefficient C_c = 1.9 of loess belong to well-graded soil, but the clay content (e.g., in silt, the part with particle size less than 0.005 mm is generally called clay.) is less than 10%. Although the gradation of loess is good, the particle size range is relatively narrow. Studies have found that liquefaction usually occurs when the clay content in silt (including loess) is less than 10% (Ministry of Housing and Urban-Rural Construction of PRC, 2016). There are also kinds of literature showing that saturated loess with a clay content of less than 12% or 15% has liquefaction behavior (Dong and Xia, 2016; He et al.,2020). The infiltration and liquefaction characteristics of loess provide favorable conditions for the occurrence of piping.

Shear Properties

In order to understand the shear characteristics of the filled loess and master the mechanical behavior of the loess comprehensively, the gradual infiltration of the dam body in the case of damage or welding gap of geomembrane or geotechnical blanket is a saturated undrained process until piping and dam break are formed. **Figure 8** compares filled loess's undrained triaxial shear test results under two different confining pressures (100–200 kPa). **Figures 8A,B** shows the variation of deviatoric stress and pore water pressure with axial strain. **Figure 8C** depicts the effective stress path. Loess samples show significant softening behavior under excess pore water pressure, and the strength decreases significantly after peak value. This deformation characteristic of loess is similar to the static liquefaction phenomenon of loose sand (He et al., 2020; Liu et al., 2020). The so-called static liquefaction refers to the apparent strain-softening phenomenon in the partial stress-strain curve of the soil sample during loading. After the peak value, the partial stress decreases sharply and approaches zero or

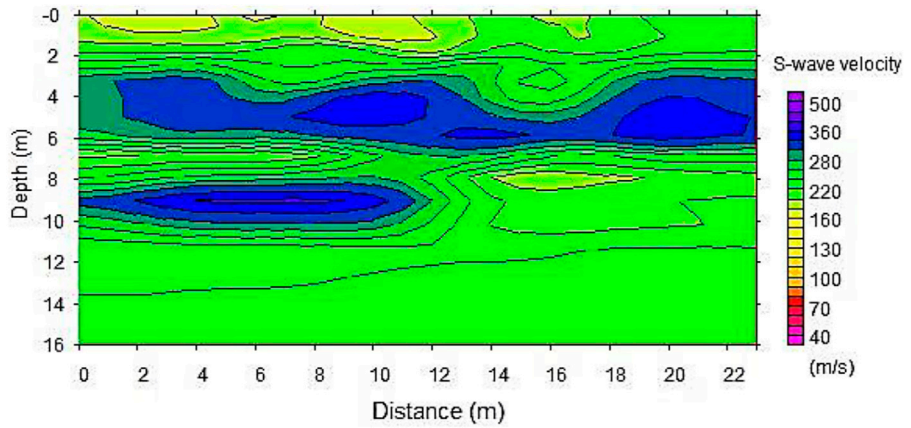

FIGURE 6 | Contour of spacing, depth, and wave velocity on longitudinal section.

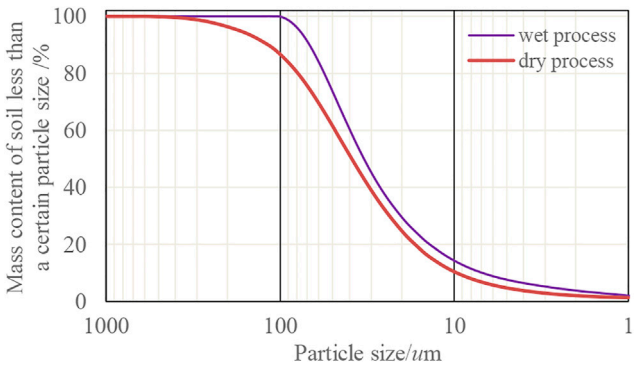

FIGURE 7 | Particle size grading curve of loess.

insufficient residual strength. The soil shows characteristics similar to fluid. **Figure 8A** is approximately consistent with the concept of static liquefaction; when the loess is saturated, the upper soil body has a loading effect on the lower soil body, and the lower saturated loess soon reaches its peak strength. When the excess pore water pressure does not increase and is almost equal to the confining pressure, the shear strength of the loess gradually decreases to the residual strength to achieve static liquefaction. These results are consistent with the Loess test results of sale mountain (Zhang et al., 2021d). Therefore, it is vital to evaluate the mechanical properties of the filled loess of the Yang village reservoir dam.

It can be seen from **Figure 8A** that the deviatoric stress peaks when the strain is minimal, and the corresponding peaks at 100 and 200 kPa are 61 and 114 kPa, respectively, and shear strength is relatively low. With the increase in the shear strain, the deviatoric stress decreases continuously from the peak value, and when the strain is significant, the deviatoric stress gradually tends to be around 25 kPa. According to the experiment, it can be seen that the residual strength of loess is deficient, showing the phenomenon of static liquefaction. The loess quickly breaks down undersaturation and deviatoric stress, further illustrating the anti-seepage arrangement's importance. It can be seen from **Figure 8B** that the development of excess static pore water pressure develops very fast at minor strains, and the development of pore water pressure begins to slow down when the strain is 3%, and finally, develops to 92 and 189 kPa. The pore water pressure and the ratios of confining pressure reached 92 and 94.5%, respectively, which were almost equal to the confining pressure, and the effective stress was already very low. From **Figure 8C**, it can be found that the effective stress path of loess has been moving towards the stress origin along with the critical state line CSL after reaching the peak value, which also reflects the same static liquefaction trend as **Figure 8A**.

DISCUSSIONS

Natural Characteristics and Approximate Static Liquefaction of Loess

The spatial variability of the Quaternary Holocene loess is enormous, and the geological environment of the Yang village reservoir is typical of silty loess with strong permeability, collapsibility, and water sensitivity. Whether it is used as an engineering foundation or dam filling material, water damage to the soil should be avoided as much as possible. As a filling material for the dam body, the management of the construction process of the dam bottom, the dam body compactness, and the construction quality of anti-seepage materials such as High-Density Polyethylene (HDPE) composite geomembrane should be strengthened, as follows:

1) The compactness of the dam bottom and the dam body should be checked layer by layer to ensure that the compactness is above 95%.
2) It is ensured that the dam bottom and body are free of unevenness, thorn particles, hard debris, etc.
3) The laying of HDPE should extend from the lowest part to the high position, do not pull too tight, to reduce the damage caused by the drag of the bentonite blanket on the foundation.

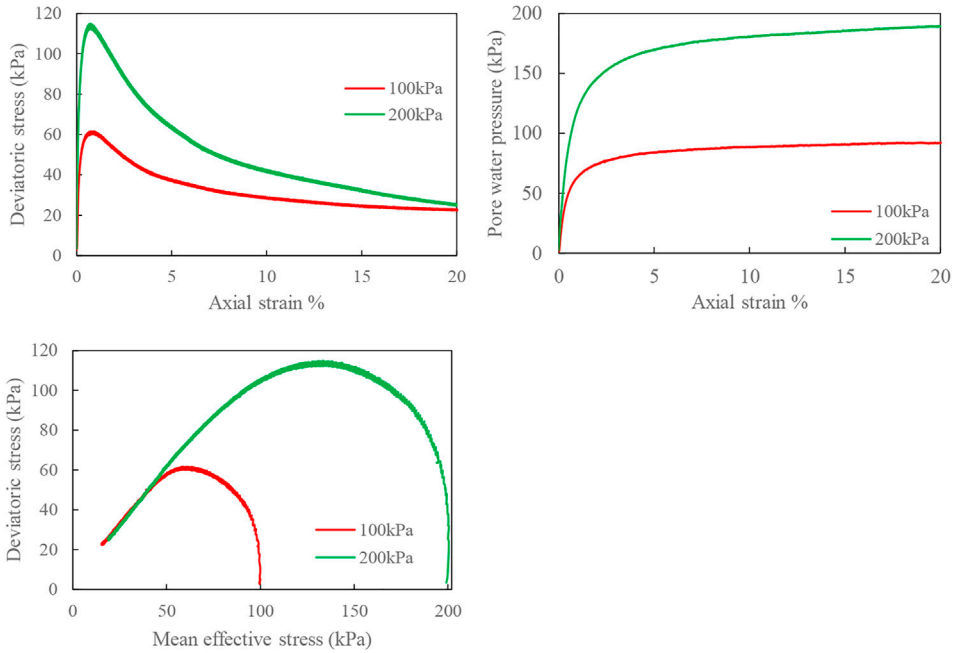

FIGURE 8 | Stress–strain relationship, pore water pressure development, and the effective stress path in loess.

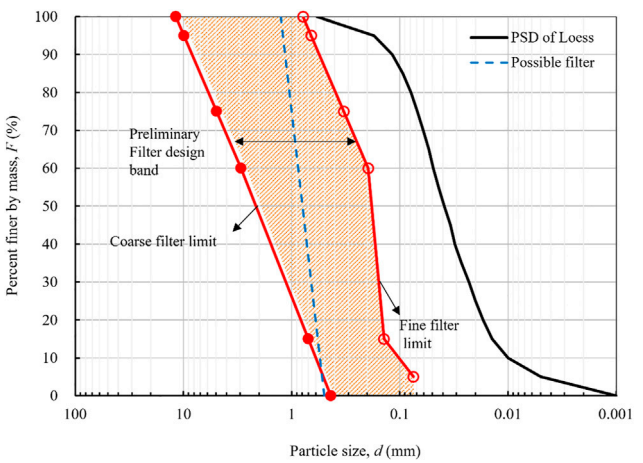

FIGURE 9 | The preliminary filter material design method.

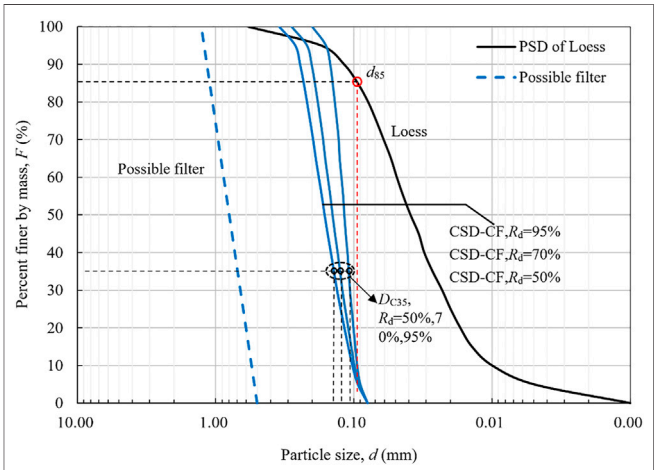

FIGURE 10 | The compaction verification of chosen filter using the CSD method.

4) Double-pass weld joints should be used in laying to reduce the number of welds, and the welding quality of the welds should be inspected in time to reduce leakage hazards. When there is a T-shaped seam, the base material is used to fill the scar, and the corners of the scar are rounded.
5) The dam body may settle under the action of the water body and its weight, and the sealing welding should also be designed to be flexible to allow vertical movement.

Suggestions on Filter Layer Design

There are three main internal erosion processes that can initiate dam failure (e.g., collapse): backward erosion, concentrated leak, and suffusion (Fell and Fry, 2007). Concentrated leakage is the main reason causing seepage failure in the embankment dams with cohesive soils, which appears in the defects (e.g., cracks, micro-fissures, and hydraulic fracture) of such structures. From the above analysis of field inspections and laboratory tests, this study concerned about the internal erosion in concentrated leaks initiated by the dam collapse. Some important physical parameters such as density, compactness, particle size distribution, fine content, and shear strength have an effect on the internal erosion properties and talked above. The most effective prevention and control measure are reasonably

installing inverted filters for the embankment dams. This study puts a particular emphasis on the design of the filter layer of loess embankment dams.

According to the characteristics of shear strength of loess in Ningxia and the potential of static liquefaction trend, a good filter design for loess will help the geotechnical and hydraulic structures in the Ningxia area maintain safety. Based on the field exploration and laboratory test results, the main reason that caused the Yang village dam break is that the internal erosion caused seepage failure because of water storage. So, the internal erosion caused potential risks should be paid special attention to this water storage structure in the loess area and filter design. Based on the current filter design theory, a well-designed filter can protect the base soil, which relates to the filter and base soil material, the hydraulic condition and the pressure acting on the base soil-filter system, shear strength of base soil, and filter soil (Zhang et al., 2021a). However, there is no filter design method related to loess. The loess soil is a kind of cohesive soil, and the cohesive soil has the ability of self-filtration (Locke and Indraratna, 2002), an improved design method of filter gradation band curves are chosen for the preliminary design of filter soils. In addition, there is an excellent possibility of dispersion for loess (Vakili et al., 2015), so the compaction of filter and base soil and other special measures should be considered for the filter design of loess.

Based on the above-mentioned analysis, a coupled design method is proposed, containing two parts. First, a filter gradation band curves design method is introduced considering the self-filtration index of loess (Zhang et al., 2021b), The preliminary filter band can be designed for the chosen filter soil; Second, a constriction size distribution (CSD) based method (Vakili et al., 2015) is chosen considering the compaction of loess and the chosen filter and the potential characteristic of dispersion. (Vakili et al., 2015), and can be used for dispersive cohesive soils, which shows as follows: $D_{15f} \leq 0.28mm$, when fine content F = 40~85%, with dispersive percent larger than 65%; $D_{c35}/d_{85}^{*} \leq 1.0$, when fine content F = 40~85%, with no dispersion; $D_{c35}/d_{85}^{*} \leq 1.25$, when fine content F ≥ 85%, with no dispersion, where, D_{15f} means the size of filter material of which 15% mass passes; D_{c35} constriction size whereby 35% of filter constriction is finer than this; d_{85}^{*} means d85 size calculated using modified PSD curve by neglecting base soil particles larger than D_{c95}; D_{c95} has the similar meaning as D_{c35}.

The coupled filter design method for loess is used in the Yang village dam, where the particle size distribution (PSD) of loess (**Figure 7**) is chosen as an example to verify the proposed method. The process of the proposed method is divided into two steps. First, the possible filter design band curves are designed using the Zhang et al. method (**Figure 9**). Second, determine the compaction and dispersive condition by choosing a possible filter in the design band curves (**Figure 10**). **Figure 9**, possible filter material chosen band intuitively displayed in **Figure 9**, we can choose one filter PSD for further compaction and dispersion verification. Finally, the chosen possible filter PSD in **Figure 8** works well when its compaction exceeds 50% (relative density greater than 50%). **Figure 10**. The above-mentioned analysis shows that the proposed filter design method for loess can work well, which can be a reference for the study of internal erosion caused failure problems in loess areas.

CONCLUSION

When the silty loess leaks in the anti-seepage materials such as the dam body's composite geomembrane, water forms the most explicit infiltration path in the silty loess, and the strength of loess is almost entirely lost, causing rapid dam failure and vast loss of life and property. We investigated a small reservoir in a typical silty loess area in Ningxia, China. The dam failure accident of this reservoir formed a typical case study of silty loess filling dam materials. In addition, the MASW survey confirmed that it could be used as a dam bottom and method for the detection of dam compactness.

Our triaxial shear tests show that the loess exhibits a near-static liquefaction phenomenon under undrained conditions, and the strength of silty loess quickly peaks with increasing strain and then gradually softens, forming a mud-like non-Newtonian fluid. Among them, the excess static pore water pressure and the effective stress path directly indicate the poor engineering properties of saturated loess (U.S. National Committee of ICOLD, 2013).

DATA AVAILABILITY STATEMENT

The original contributions presented in the study are included in the article/Supplementary Materials, further inquiries can be directed to the corresponding author.

AUTHOR CONTRIBUTIONS

GZ provided a scientific design of an inverted filter for filling materials of loess dam. The authors express their sincere gratitude to YZ and QL of Ningxia University for invaluable assistance in the field investigation.

FUNDING

This work was supported by the National Natural Science Foundation of China (NSFC), Grant/Award Nos: 51768059 and 11662015, and the Natural Science Foundation of Ningxia Province, Grant/Award No: 2022AAC03106.

ACKNOWLEDGMENTS

The first author's special thanks go to Lei Wang, Earth Products China Limited (EPC), who actively carried out surface wave tests on site. This company was not involved in the study design, collection, analysis, interpretation of data, the writing of this article or the decision to submit it for publication. The first author is particularly grateful to PW and YY for giving helpful guidance in surface wave measurement, triaxial test, and particle size analysis.

REFERENCES

ASTM. (2020). Standard Test Method for Consolidated Undrained Triaxial Compression Test for Cohesive Soils. Available at: https://www.astm.org/standards/d4767, pp.1–14. doi:10.1520/D4767-11R20

Boss International (1999). *BOSS DAMBRK Hydrodynamics Flooding Routing User's Manual*. Madison, USA: Wiscosin.

Dong, L. L. M., and Xia, K. (2016). Two Discoveries in the Liquefaction Evaluation Method of Saturated Loess. *China Earthq. Eng. J.* 38 (5), 770–774. doi:10.3969/j.issn.1000-0844.2016.05.0770

Fell, R., and Fry, J. J. (2007). *Internal Erosion of Dams and Their Foundations: Selected Papers from the Workshop on Internal Erosion and Piping of Dams and Their Foundations*. London: Taylor & Francis.

Harba, P., Pilecki, Z., and Krawiec, K. (2019). Comparison of MASW and Seismic Interferometry with Use of Ambient Noise for Estimation of S-Wave Velocity Field in Landslide Subsurface. *Acta Geophys.* 67 (6), 1875–1883. doi:10.1007/s11600-019-00344-9

He, S., Wang, X., Fan, H., Wang, H., Ren, R., and Guo, C. (2020). The Study on Loess Liquefaction in China: a Systematic Review. *Nat. Hazards* 103, 1639–1669. doi:10.1007/s11069-020-04085-7

International Commission on Large Dams (ICOLD) (2021). Dam Safety Management: Pre-operational Phases of the Dam Life Cycle. *Bulletin* 175. London: CRC Press. doi:10.1201/9781003169482

Islam, T., and Chik, Z. (2011). Advanced Performance in Geotechnical Engineering Using Tomography Analysis. *Environ. Earth Sci.* 63 (2), 291–296. doi:10.1007/s12665-010-0702-4

Ismail, A., Brett Denny, F., and Metwaly, M. (2014). Comparing Continuous Profiles from MASW and Shear-Wave Reflection Seismic Methods. *J. Appl. Geophys.* 105, 67–77. doi:10.1016/j.jappgeo.2014.03.007

Jiang, J., and Yang, Z. (2008). Laws of Dam Failures of Small-Sized Reservoirs and Countermeasures. *Chin. J. Geotechnical Eng.* 30(11),1626–1631.

Karray, M., and Lefebvre, G. (2009). Détection des cavités sous les pavages par l'analyse modal des ondes de Rayleigh (MASW). *Can. Geotech. J.* 46 (4), 424–437. doi:10.1139/T09-009

Khan, Z., and Yamin, M. (2019). Evaluation of Shear Geophones in MASW Testing. *Int. J. Geotechnical Eng.* 13 (2), 184–190. doi:10.1080/19386362.2017.1329260

Kho, F. W., Law, P. L., Lai, S. H., Oon, Y. W., Ngu, L. H., and Ting, H. S. (2009). Quantitative Dam Break Analysis on a Reservoir Earth Dam. *Int. J. Environ. Sci. Technol.* 6 (2), 203–210. doi:10.1007/bf03327623

Liu, W., Chen, W., Wang, Q., Wang, J., and Lin, G. (2020). Effect of Pre-dynamic Loading on Static Liquefaction of Undisturbed Loess. *Soil Dyn. Earthq. Eng.* 130. 105915. doi:10.1016/j.soildyn.2019.105915

Locke, M., and Indraratna, B. (2002). Filtration of Broadly Graded Soils: the Reduced PSD Method. *Géotechnique* 52 (4), 285–287. doi:10.1680/geot.2002.52.4.285

Luo, Y, Chen, L., Xu, M., and Tong, X. (2012). Review of Dam-Break Research of Earth-Rock Dam Combining with Dam Safety Management. *Procedia Eng.* 28, 382–388. doi:10.1016/j.proeng.2012.01.737

Ministry of Housing and Urban-Rural Construction of PRC (2016). *GB 50011-2010, Code for Seismic Design of Buildings*. Edition. China: China Architecture & Building Press, 23–25.

Ministry of Water Resources of PRC (2021). *River Management in the Chinese Water Statistical Yearbook*. Beijing: China Water & Power Press, 30–52.

Ministry of Water Resources of PRC (2017). *SL258-2017, Guidelines on Dam Safety Evaluation*, 37–42. Beijing: China Water & Power Press.

Morris, M. W., Hassan, M. A. A. M., and Vaskinn, K. A. (2007). Breach Formation: Field Test and Laboratory Experiments. *J. Hydraulic Res.* 45 (2S), 9–17. doi:10.1080/00221686.2007.9521828

Nabilah, R. A., Sutjiningsih, D., Sutjiningsih, D., Anggraheni, E., and Murniningsih, S. 2020). Dam Break Analysis of Situ Gintung Dam Collapse Reconstruction, *IOP Conf. Ser. Earth Environ. Sci.*, 599, 012064. doi:10.1088/1755-1315/599/1/012064

Pilotti, M. A., Maranzoni, A., Tomirotti, M., and Valerio, G. (2011). 1923 Gleno Dam Break: Case Study and Numerical Modeling. *J. Hydraul. Eng.* 137 (4), 480–492. doi:10.1061/(asce)hy.1943-7900.0000327

The Australian National Committee on Large Dams Incorporated (2020). *Guidelines on the Consequence Categories for Dams (Reprint with Amendments)*. Tasmania: Hobart.

U.S. National Committee of ICOLD (2013). *Dams of the United States-A Pictorial Display of Landmark Dams*. Colorado: U.S. Society of Dams.

Vakili, A. H., Bin Selamat, M. R., and Abdul Aziz, H. bin. (2015). Filtration of Broadly Graded Cohesive Dispersive Base Soils. *J. Geotechnical Geoenvironmental Eng.* 141 (5), 1–12. doi:10.1061/(asce)gt.1943-5606.0001280

Wang, Z. Y., Chen, Z. Y., Yu, S., Zhang, Q., Wang, Y., and Hao, J. W. (2021a). Erosion-control Mechanism of Sediment Check Dams on the Loess Plateau. *Int. J. Sediment Res.* 36 (5), 668–677. doi:10.1016/j.ijsrc.2021.02.002

Wang, H., Wang, Y. Z., Tang, Z. G., Yuan, X. M., and Duan, X. F. (2021b). Shear Wave Velocity-Relative Density United Tests and Verification of Empirical Formula. *Chin. J. Undergr. Space Eng.* 17 (6), 1881–1887.

Wu, S. (2020). Statistics and Analysis of Dam Failures in United States since 2010. *Dam Saf.* 5, 61–65. doi:10.3969/j.issn.1671-1092.2020.05.017

Xie, J. B., and Sun, D. Y. (2009). Statistics of Dam Failures in China and Analysis on Failure Causations. *Water Resour. Hydropower Eng.* 40 (12), 124–128. doi:10.3969/j.issn.1000-0860.2009.12.032

Xu, J., Wei, W., Bao, H., Zhang, K., Lan, H., Yan, C., et al. (2020). Failure Models of a Loess Stacked Dam: a Case Study in the Ansai Area (China). *Bull. Eng. Geol. Environ.* 79 (2), 1009–1021. doi:10.1007/s10064-019-01605-z

Xu, J., Wei, W., Bao, H., Zhang, K., Lan, H., Yan, C., et al. (2020). Study on Shear Strength Characteristics of Loess Dam Materials under Saturated Conditions. *Environ. Earth Sci.* 79 (13). doi:10.1007/s12665-020-09089-x

Zhang, Z., Chai, J., Li, Z., Xu, Z., and Yuan, S. (2021a). Reconstruction and Effects of a Failure of a Typical Check Dam System under an Extreme Rainstorm on the Loess Plateau, China. *Nat. Hazards* 111, 1401–1419. doi:10.1007/s11069-021-05101-0

Zhang, G., Wang, H. Y., and Jahanzaib, I. (2021b). Improved Design Method of Gradation Band Curves for Granular Filters. *Shuili Fadian Xuebao/Journal Hydroelectr. Eng.* 40 (4), 73–83. doi:10.11660/slfdxb.20210408

Zhang, G., Israr, J., Ma, W., and Wang, H. (2021c). Modeling Water-Induced Base Particle Migration in Loaded Granular Filters Using Discrete Element Method. *Water* 13 (14), 1976. doi:10.3390/w13141976

Zhang, F., Peng, J., Wu, X., Pan, F., Jiang, C., et al. (2021d). A Catastrophic Flowslide that Overrides a Liquefied Substrate: the 1983 Saleshan Landslide in China. *Earth Surf. Process. Landforms* 46 (10), 2060–2078. doi:10.1002/esp.5144

Zhao, T. L., Chen, S. S., Fu, C. J., and Zhong, Q. M. (2019). Centrifugal Model Tests and Numerical Simulations for Barrier Dam Break Due to Overtopping. *J. Mt. Sci.* 16 (3), 630–640. doi:10.1007/s11629-018-5024-0

Zhong, D., Sun, Y., and Li, M. (2011). Dam Break Threshold Value and Risk Probability Assessment for an Earth Dam. *Nat. Hazards* 59 (1), 129–147. doi:10.1007/s11069-011-9743-6

Conflict of Interest: The authors declare that the research was conducted in the absence of any commercial or financial relationships that could be construed as a potential conflict of interest.